Periodontitis

Jaewoong Lee   Seunghoon Kim   Semin Lee

2020-12-03

Contents

List of Tables

List of Figures

1 Introduction

1.1 Microbiome

Microbiome is consist of microbiota, the micro-organisms which live inside and on humans (Turnbaugh et al., 2007). Microbiome is also about 10^{13} micro-organisms whose which collective genome (Gill et al., 2006).

1.2 Ribosomal RNA

Ribosomal RNA (rRNA) is well-known as a key to phylogeny (Olsen & Woese, 1993).

1.3 16S rRNA Gene Sequencing

1.4 Periodontitis

Periodontitis is an inflammatory conditions which effecting periodontium, tissues which surround and support teeth. Major components of periodontitis are clinical attachment loss and bone loss (Flemmig, 1999). Previous study found risk factors of periodontitis such as smoking, diabetes, genetic factors and host response (Van Dyke & Dave, 2005).

2 Materials

2.1 16S rRNA Gene Sequencing

- 100 Healthy samples
- 50 Chronic Early Periodontitis Sample
- 50 Chronic Moderate Periodontitis Sample
- 50 Chronic Severe Periodontitis Sample

3 Methods

3.1 QIIME2 Workflow

QIIME2 is a capable, expandable and distributed microbiome analysis package with transparent analysis (Bolyen et al., 2019, 2018). A theoretic overview of QIIME2 workflow is shown as figure 2.

3.1.1 Denoising techniques

There are two denoising techniques provided by QIIME2: DADA2 (Callahan et al., 2016) and Deblur (Amir et al., 2017). Major difference between DADA2 and Deblur, as shown as figure 3, is a strategy, the strategy used to divide as different species. DADA2 uses amplicon sequence variants (ASVs), strictly divides sequences even one-base mismatch. However, Deblur uses operational taxonomic units (OTUs), considers as same sequence when sequences are 97 % or more matched.

3.1.2 Taxonomy Classification

There are two taxonomy classification databases which provided by QIIME2: Greengenes (GG) (DeSantis et al., 2006) and SILVA (Pruesse et al., 2007). Major difference between Greengenes and SILVA is resolution. Resolution of Greengenes is from kingdom to species; however, resolution of SILVA is from domain to genus. Note that a higher accuracy at taxonomic levels above genus level; but accuracy drops at species level (Gihawi et al., 2019).

3.1.3 Merging Denoising and Taxonomy Classification

After denosing and taxonomy classification steps, some different IDs (ASVs or OTUs) have been identified as same taxonomy. In that case, the different IDs will be merged into one taxonomy (Figure 5).

3.1.4 Rarefaction

Rarefaction is a statistical method of estimating the number of species expected in a random sample which taken from a collection (James & Rathbun, 1981). Moreover, rarefaction allows comparisons of the species richness among communities. Thus, rarefaction is a good choice for normalization (Weiss et al., 2017).

Figure 1: Concept of a Core Human Microbiome (Turnbaugh et al., 2007)

Figure 2: A Theoretic Overview of QIIME2 Workflow (Bolyen et al., 2019, 2018)
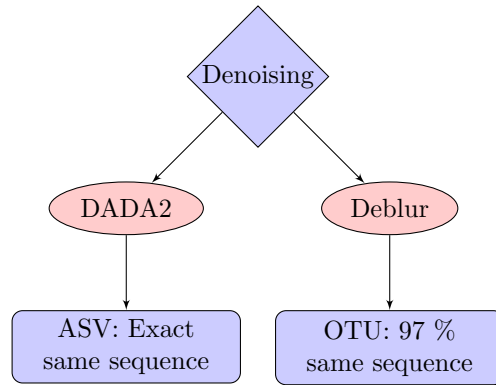
Figure 3: Denoising Techniques which provided by QIIME2
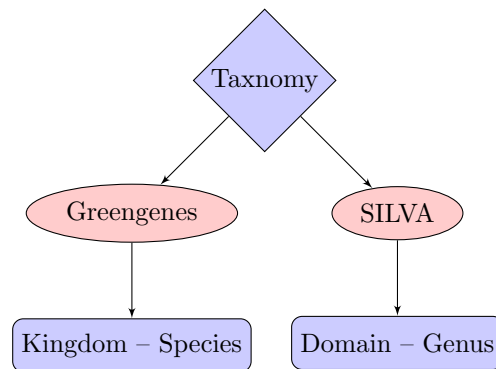
Figure 4: Taxonomy Classification which provided by QIIME2
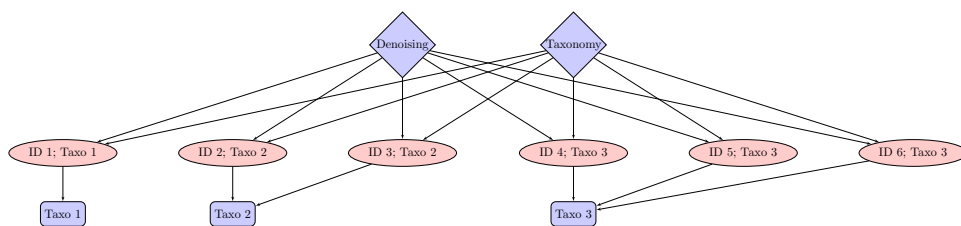
Figure 5: Example Diagram for Merging Denoising and Taxonomy Classification

3.1.5 Alpha-diversity

Alpha-diversity is a metric which shows the richness of taxa at a single community. There are four alpha-diversity indices which provided from QIIME2:

- Evenness index.

- Faith's phylogenetic diversity (Faith PD).

- Observed features.

- Shannon's diversity index.

Shannon's diversity index shows a quantitative measure of community richness; Observed features, however, is a qualitative measure of community richness. Faith's phylogenetic diversity index indicates a qualitative measure of community richness which assimilates phylogenetic relationship among features. Finally, evenness index, as its name, shows a measure of community evenness.

3.1.6 Beta-diversity

Beta-diversity is a metric which indicates the taxonomic differentiation between multiple communities. There are four beta-diversity indices which provided from QIIME2:

- Bray-Curtis distance.

- Jaccard distance.

- Unweighted UniFrac distance.

- Weighted UniFrac distance.

Bray-Curtis distance shows a quantitative of community dissimilarity; Jaccard distance, however, indicates a qualitative measure of community dissimilarity. UniFrac distances reveal a measure of community dissimilarity which consolidates phylogenetic relationship among features. Difference between unweighted UniFrac distance and weighted UniFrac distance is a qualitative and a quantitative, respectively.

3.1.7 ANCOM

ANCOM (Analysis of composition of microbiomes) can be used for analyzing the composition of microbiome in multiple populations (Mandal et al., 2015). Example ANCOM volcano plot is shows as figure 6. In figure 6, two metrics are clearly shown: clr and W. clr stands for centered log ratio, and W is a count of the number of sub-hypothesis which have passed for given species.

3.2 Python Packages

3.2.1 Pandas

Pandas is a Python package of rich data structures and tools for analyzing with structured data sets (McKinney et al., 2011).

3.2.2 Scikit-learn

Scikit-learn grants state-of-the-art implementation of many machine learning algorithms, while controlling an easy-to-use interface tightly integrated the Python code (Pedregosa et al., 2011).

3.2.3 Matplotlib

Matplotlib is a Python graphics package which used for application development, interactive scripting and publication quality image generation (Barrett, Hunter, Miller, Hsu, & Greenfield, 2005). Matplotlib, also, is designed to create simple plots with a few commands (Hunter, 2007).

3.2.4 Seaborn

Seaborn is a Python data visualization package which based on matplotlib, allows a high-level interface for displaying engaging and descriptive statistical graphics (Waskom & the seaborn development team, 2020).

3.3 t-SNE

t-SNE (t-distributed stochastic neighbor embedding) reveals high-dimensional data a location in two-dimensional map (Maaten & Hinton, 2008). Figure 7 is example of t-SNE with hand-writing digits (Maaten & Hinton, 2008). In figure 7, all 10 digits are grouped into 10 groups clearly; some hand-writings, however, are classified into wrong groups due to their similar shapes, such as 0 and 6.

3.4 Classification

In machine learning, Classification is one of supervised learning which identifies a class of a new observation, depends on given information which consist of training observations and their classes.

In this study, classification will be carried out as figure 8; and the third step in figure 8 is demonstrated in minute detail as figure 9. Note that the first step in figure 8 is optional: due to tables herein-after, such as table2, show that no statistically significant differences between healthy samples and early periodontitis samples and between moderate periodontitis samples and severe periodontitis samples.

Moreover, in this study, followed classification algorithms are used:

- RandomForest Classification Algorithm (Breiman, 2001; Pedregosa et al., 2011)

4 Results

4.1 Quality Filter

Longer sequences have more fallen sequence quality than shorter. Thus, sequences which longer than threshold should be trimmed out due to their low quality. However, gold-standard strategy for deciding the threshold does not exist; the threshold is set as longest sequence length which have half of sequences have greater than 30 quality score. Hence, sequence quality plot is shown as figure 10; trimmed length in forward reads is 300, and trimmed length in reverse reads is 265.

4.2 Rarefaction

Sampling depth should be decided for rarefaction. Gold-standard method for determining sampling depth is minimum frequency in the samples. Hence, sampling depth with DADA2 is 3786 (Figure 11), and sampling depth with Deblur is 7253 (Figure 12).

4.3 Alpha-diversity

Alpha-diversity analysis with DADA2 was done: Evenness index (Table 2 and Figure 13), Faith PD (Table 3 and Figure 14), observed feature index (Table 4 and Figure 15) and Shannon's diversity index (Table 5 and Figure 16). Also, alpha-diversity analysis with DADA2 was done: Evenness index (Table 7 and Figure 17), Faith PD (Table 8 and Figure 18), observed feature index (Table 9 and Figure 19) and Shannon's diversity index (Table 10 and Figure 20). Moreover, Kruskal-Wallis tests among all groups are shown as table 1 (with DADA2) and table 6 (with Deblur).

4.4 Beta-diversity

Beta-diversity analysis with DADA2 was done: Bray-Curtis distance (Table 11 and Figure 21), Jaccard distance (Table 12 and Figure 22), unweighted UniFrac distance (Table 13 and Figure 23) and weighted UniFrac distance (Table 14 and Figure 23). Also, beta-diversity analysis with Deblur was done: Bray-Curtis distance (Table 15 and Figure 25), Jaccard distance (Table 16 and Figure 26), unweighted UniFrac distance (Table 17 and Figure 27) and weighted UniFrac distance (Table 18 and Figure 27).

4.5 ANCOM

Statistically significant different taxa and volcano plots by ANCOM were derived: DADA2 and Greengenes (Table 19 and Figure 29), DADA2 and SILVA (Table 20 and Figure 30), Deblur and Greengenes (Table 21 and Figure 31) and Deblur and SILVA (Table 22 and Figure 32).

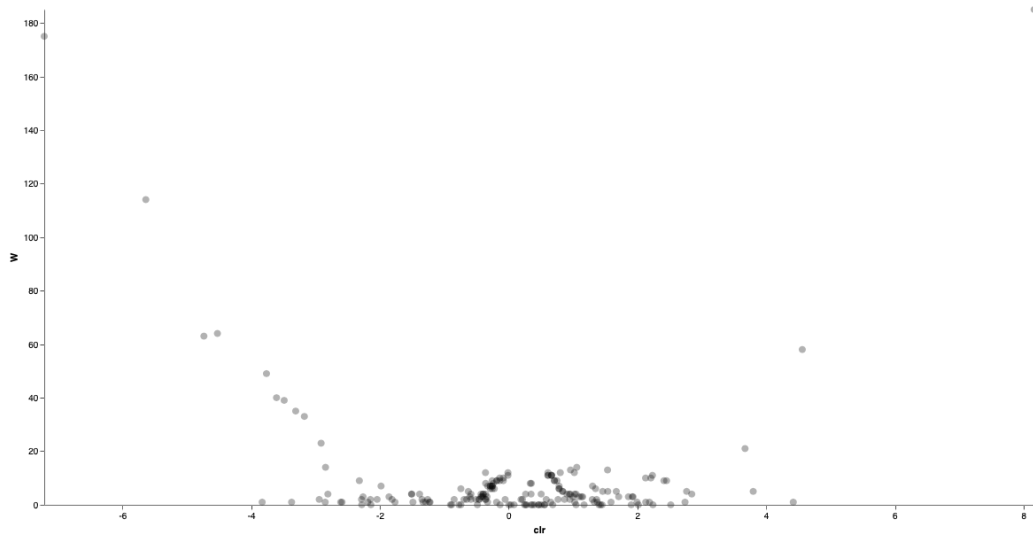Figure 6: Example ANCOM Volcano Plot which Provided by QIIME2 (Bolyen et al., 2019, 2018)
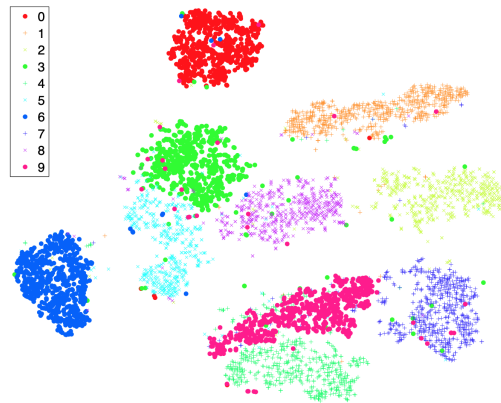

Figure 7: Visualization by t-SNE (Maaten & Hinton, 2008)

Figure 8: Workflow of Classification
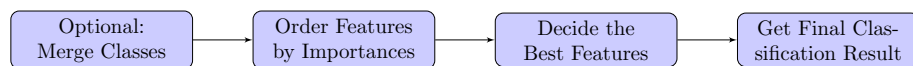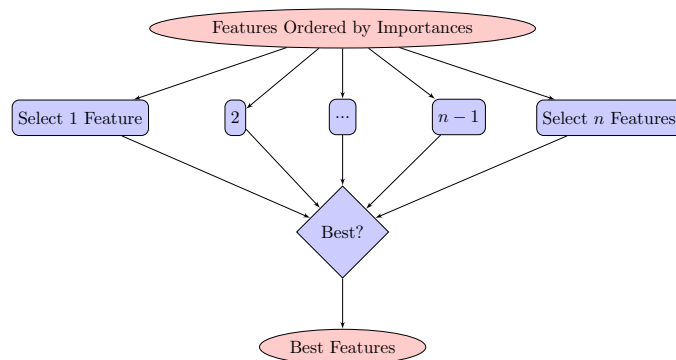

Figure 9: Deciding the Best Features

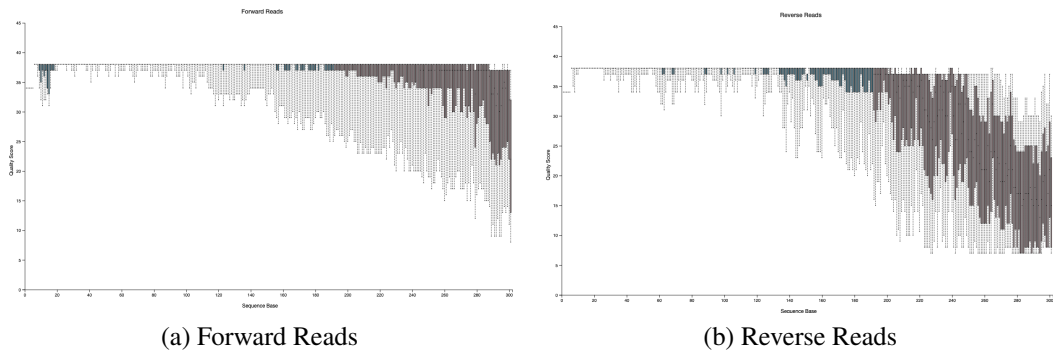(a) Forward Reads   (b) Reverse Reads
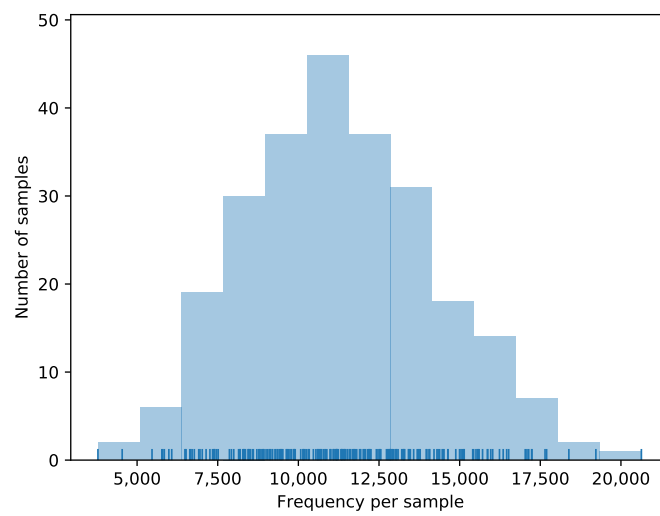
Figure 10: Sequence Quality Plot
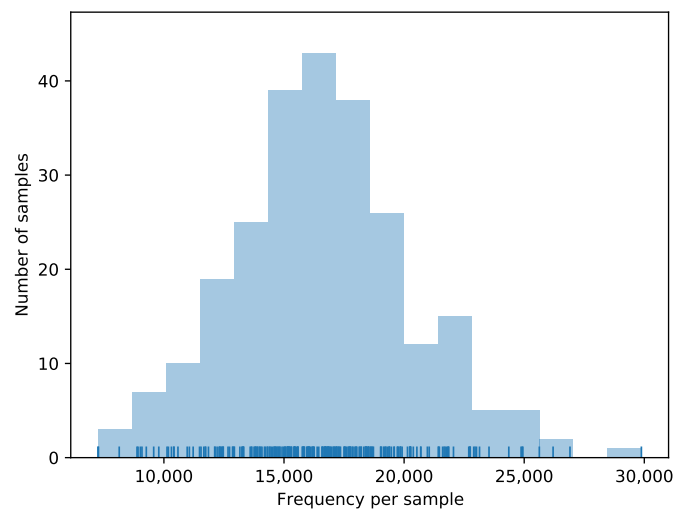

Figure 11: Frequency and Number per Sample by DADA2

Figure 12: Frequency and Number per Sample by Deblur

Table 1: Kruskal-Wallis Tests among All Group with DADA2

Alpha-Diversity	H	p-value
Evenness	12.185457848605665	0.006774123738087294
Faith PD	33.42272318725111	2.6227945981005624e-7
Observed Features	21.019370066584198	0.0001043055436502384
Shnnon's Diversity	7.311350438247132	0.06260902704190516

Table 2: Kruskal-Wallis Tests from Evenness Index with DADA2

Group 1	Group 2	H	p-value	q-value
Early (n=50)	Healthy (n=100)	0.003576158940404639	0.9523141335184352	0.9523141335184352
Early (n=50)	Moderate (n=50)	5.112902970297	0.02374855135702787	0.03562282703554181
Early (n=50)	Severe (n=50)	5.206859405940577	0.022497939047433364	0.03562282703554181
Healthy (n=100)	Moderate (n=50)	6.591830463576116	0.01024477815032801	0.03073433445098403
Healthy (n=100)	Severe (n=50)	6.756619867549659	0.0093400517403089	0.03073433445098403
Moderate (n=50)	Severe (n=50)	0.01216633663364064	0.9121705706341857	0.9523141335184352

Table 3: Kruskal-Wallis Tests from Faith PD Index with DADA2

Group 1	Group 2	H	p-value	q-value
Early (n=50)	Healthy (n=100)	0.3434543046357703	0.557842085850555	0.557842085850555
Early (n=50)	Moderate (n=50)	7.833790099009889	0.005127846488653557	0.0076917697329803355
Early (n=50)	Severe (n=50)	19.832839603960394	8.451807369366e-06	2.5355422108098e-05
Healthy (n=100)	Moderate (n=50)	8.964254304635801	0.0027531304578610103	0.005506260915722021
Healthy (n=100)	Severe (n=50)	24.32056688741727	8.156352492752821e-07	4.893811495651693e-06
Moderate (n=50)	Severe (n=50)	5.461592079207946	0.019438927334967618	0.02332671280196114

Table 4: Kruskal-Wallis Tests from Observed Features Index with DADA2

Group 1	Group 2	H	p-value	q-value
Early (n=50)	Healthy (n=100)	9.559750209810552	0.001988901703187571	0.005966705109562713
Early (n=50)	Moderate (n=50)	0.01069480203811357	0.9176330712208788	0.9176330712208788
Early (n=50)	Severe (n=50)	1.8918489487993617	0.1689935259025544	0.20279223108306527
Healthy (n=100)	Moderate (n=50)	16.280824652808626	5.461383546704547e-05	0.0003276830128022728
Healthy (n=100)	Severe (n=50)	6.9139163882453465	0.008552745576573654	0.0171054911153147308
Moderate (n=50)	Severe (n=50)	2.1161415616917054	0.145753334857958	0.20279223108306527

Table 5: Kruskal-Wallis Tests from Shannon's Diversity Index with DADA2

Group 1	Group 2	H	p-value	q-value
Early (n=50)	Healthy (n=100)	5.291586754966886	0.021428686619934936	0.11394854365524665
Early (n=50)	Moderate (n=50)	1.3095920792079028	0.2524685249140654	0.3029622298968785
Early (n=50)	Severe (n=50)	4.305790099009869	0.037982847885082216	0.11394854365524665
Healthy (n=100)	Moderate (n=50)	2.223194701986756	0.13595148461788642	0.271190296923577284
Healthy (n=100)	Severe (n=50)	0.06109668874171348	0.8047709009969876	0.8047709009969876
Moderate (n=50)	Severe (n=50)	1.3573544554455452	0.2439965042398798	0.3029622298968785

Table 6: Kruskal-Wallis Tests among All Group with Deblur

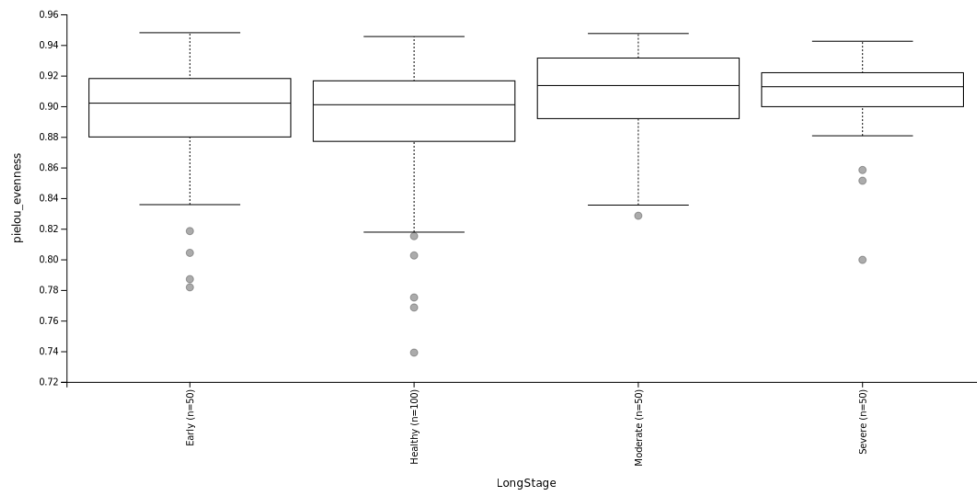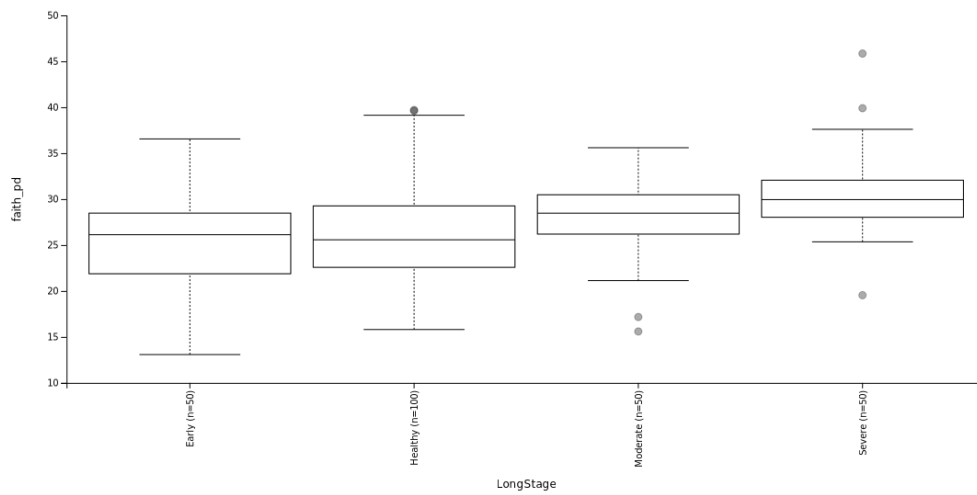| Alpha-Diversity	H	p-value
Evenness	9.242885737051779	0.026229960554059864
Faith PD	87.83605864541846	6.386769940789011e-19
Observed Features	59.59138364929631	7.186872791755095e-13
Shnnon's Diversity	24.823351075697246	0.0000168109082960023026

Figure 13: Evenness Index from DADA2
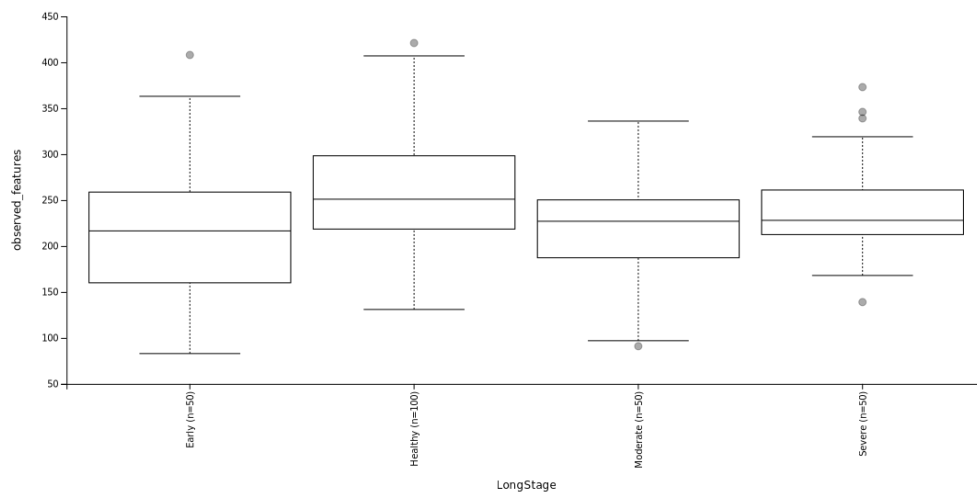

Figure 14: Faith PD Index from DADA2

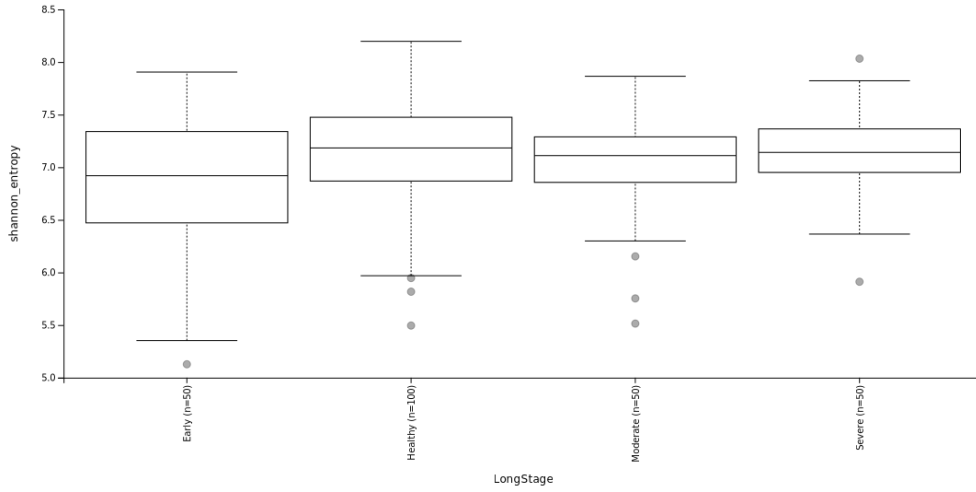Figure 15: Observed Features Index from DADA2

Figure 16: Shannon's Diversity Index from DADA2

Table 7: Kruskal-Wallis Tests from Evenness Index with Deblur

Group 1	Group 2	H	p-value	q-value
Early (n=50)	Healthy (n=100)	2.884386754966897	0.0894420544121846	0.15829564582637523
Early (n=50)	Moderate (n=50)	4.392047524752456	0.03610692636685824	0.10832077910057474
Early (n=50)	Severe (n=50)	8.828245544554477	0.002966034055389358	0.017796204332336148
Healthy (n=100)	Moderate (n=50)	0.6168317880794802	0.43222705558822094	0.43597874518665736
Healthy (n=100)	Severe (n=50)	2.6199099337748066	0.1055304305509168	0.15829564582637523
Moderate (n=50)	Severe (n=50)	0.6068435643564385	0.43597874518665736	0.43597874518665736

Table 8: Kruskal-Wallis Tests from Faith PD Index with Deblur

Group 1	Group 2	H	p-value	q-value
Early (n=50)	Healthy (n=100)	2.7110304635762077	0.09965659889456922	0.11958791867348306
Early (n=50)	Moderate (n=50)	26.80400792079206	2.251698564500841e-07	3.3775478467512613e-07
Early (n=50)	Severe (n=50)	29.06252673267329	7.007948881210323e-08	1.4015897762420645e-07
Healthy (n=100)	Moderate (n=50)	51.153949668874134	8.539868055189094e-13	2.5619604165567283e-12
Healthy (n=100)	Severe (n=50)	54.86883178807949	1.288482355374052e-13	7.730894132244311e-13
Moderate (n=50)	Severe (n=50)	0.005750495049483106	0.9395527422741722	0.9395527422741722

Table 9: Kruskal-Wallis Tests from Observed Features Index with Deblur

Group 1	Group 2	H	p-value	q-value
Early (n=50)	Healthy (n=100)	0.4675226919952207	0.49412905906624816	0.5929548708794977
Early (n=50)	Moderate (n=50)	18.684815977243918	1.542055834477253e-05	2.31308375171588e-05
Early (n=50)	Severe (n=50)	20.703272962949605	5.362426456004328e-06	1.0724852912008657e-05
Healthy (n=100)	Moderate (n=50)	35.26606516292951	2.875998708064018e-09	8.627996124192055e-09
Healthy (n=100)	Severe (n=50)	37.015293460828644	1.1720632904898772e-09	7.032379742939263e-09
Moderate (n=50)	Severe (n=50)	0.003849966992737873	0.9505245257136643	0.9505245257136643

Table 10: Kruskal-Wallis Tests from Shannon's Diversity Index with Deblur

| Group 1	Group 2	H	p-value	q-value
Early (n=50)	Healthy (n=100)	0.38679735099333357	0.5339876723058008	0.6407852067669609
Early (n=50)	Moderate (n=50)	10.767968316831627	0.0010327180791227218	0.0020654361582454436
Early (n=50)	Severe (n=50)	14.428562376237608	0.00014557751137778065	0.000627545643904027
Healthy (n=100)	Moderate (n=50)	10.172185430463571	0.0014257517732722547	0.0021386276559908382
Healthy (n=100)	Severe (n=50)	13.746754966887409	0.0002091818813013423	0.000627545643904027
Moderate (n=50)	Severe (n=50)	0.15987326732670226	0.6892732232396639	0.6892732232396639
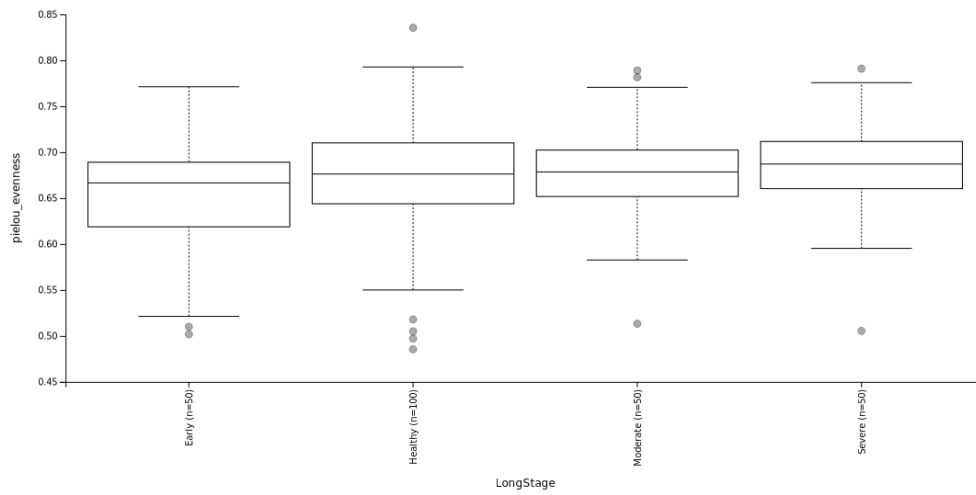
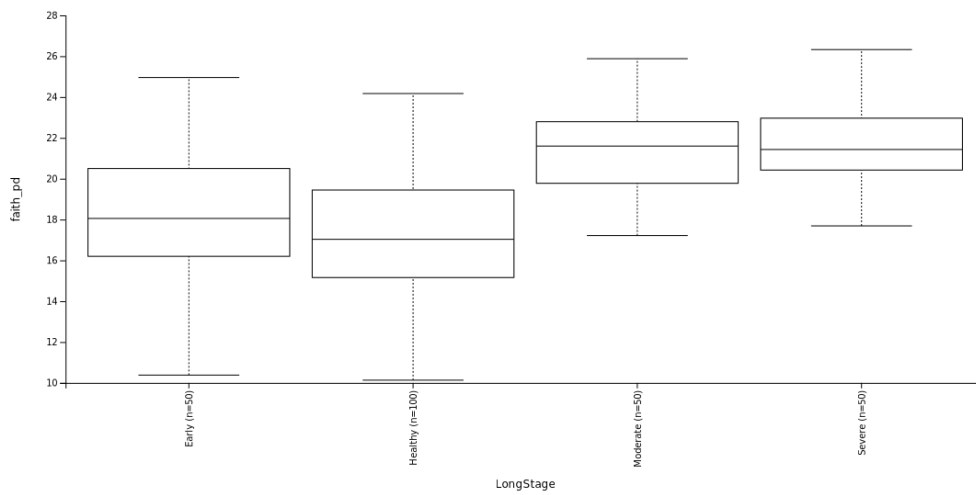Figure 17: Evenness Index from Deblur
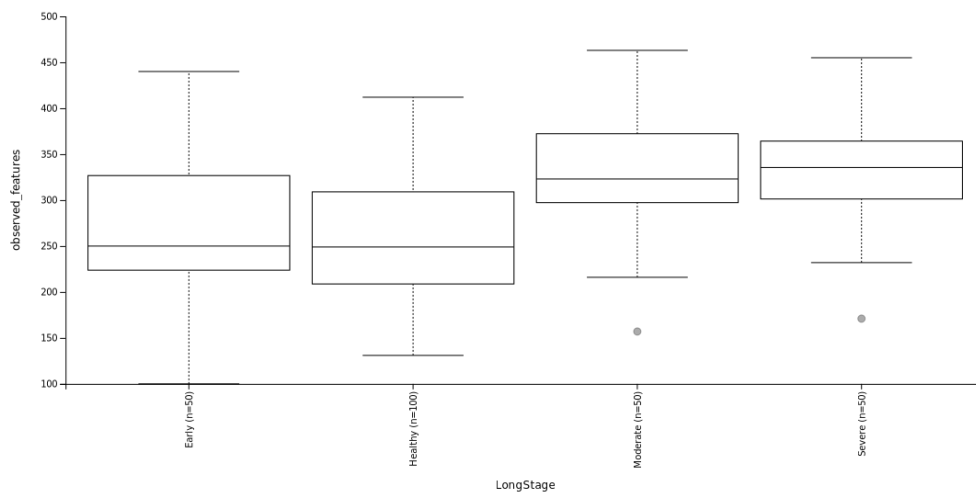

Figure 18: Faith PD Index from Deblur
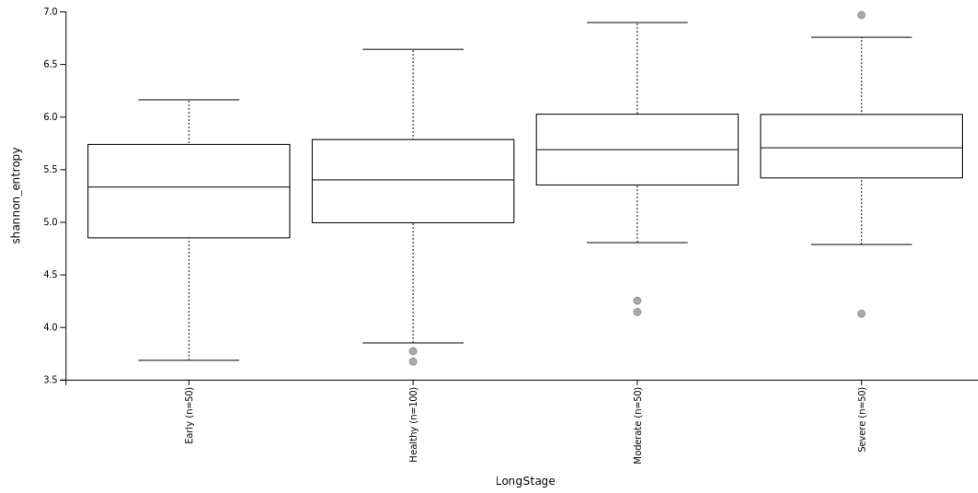

Figure 19: Observed Features Index from Deblur

Figure 20: Shannon's Diversity Index from Deblur

Table 11: Bray-Curtis Distance Index with DADA2

Group 1	Group 2	Sample size	Permutations	pseudo-F	p-value	q-value
Early	Healthy	150	999	1.8288671026193992	0.004	0.0048
Early	Moderate	100	999	2.4738348324475568	0.001	0.0015
Early	Severe	100	999	3.3691960533567005	0.001	0.0015
Healthy	Moderate	150	999	5.602936565444328	0.001	0.0015
Healthy	Severe	150	999	6.325447306476738	0.001	0.0015
Moderate	Severe	100	999	1.1018815494184453	0.219	0.219

Table 12: Jaccard Distance Index with DADA2

Group 1	Group 2	Sample size	Permutations	pseudo-F	p-value	q-value
Early	Healthy	150	999	1.5875955458962276	0.001	0.0012
Early	Moderate	100	999	1.7486415070626309	0.001	0.0012
Early	Severe	100	999	1.8371794988000507	0.001	0.0012
Healthy	Moderate	150	999	3.9547515710373635	0.001	0.0012
Healthy	Severe	150	999	3.8380356039546784	0.001	0.0012
Moderate	Severe	100	999	0.9700395015774723	0.62	0.62

Table 13: Unweighted UniFrac Distance Index with DADA2

Group 1	Group 2	Sample size	Permutations	pseudo-F	p-value	q-value
Early	Healthy	150	999	2.414078271406213	0.002	0.0024
Early	Moderate	100	999	4.941256726696032	0.001	0.0015
Early	Severe	100	999	6.184322196061149	0.001	0.0015
Healthy	Moderate	150	999	12.484494695636283	0.001	0.0015
Healthy	Severe	150	999	13.432593034368626	0.001	0.0015
Moderate	Severe	100	999	1.2428267228930112	0.084	0.084

Table 14: Weighted UniFrac Distance Index with DADA2

Group 1	Group 2	Sample size	Permutations	pseudo-F	p-value	q-value
Early	Healthy	150	999	2.6584441800971716	0.019	0.022799999999999997
Early	Moderate	100	999	8.702906307484113	0.001	0.0015
Early	Severe	100	999	14.068214366598513	0.001	0.0015
Healthy	Moderate	150	999	22.059259782524673	0.001	0.0015
Healthy	Severe	150	999	31.310013450629775	0.001	0.0015
Moderate	Severe	100	999	1.7543213081828324	0.115	0.115

(a) Healthy
(b) Early
(c) Moderate
(d) Severe
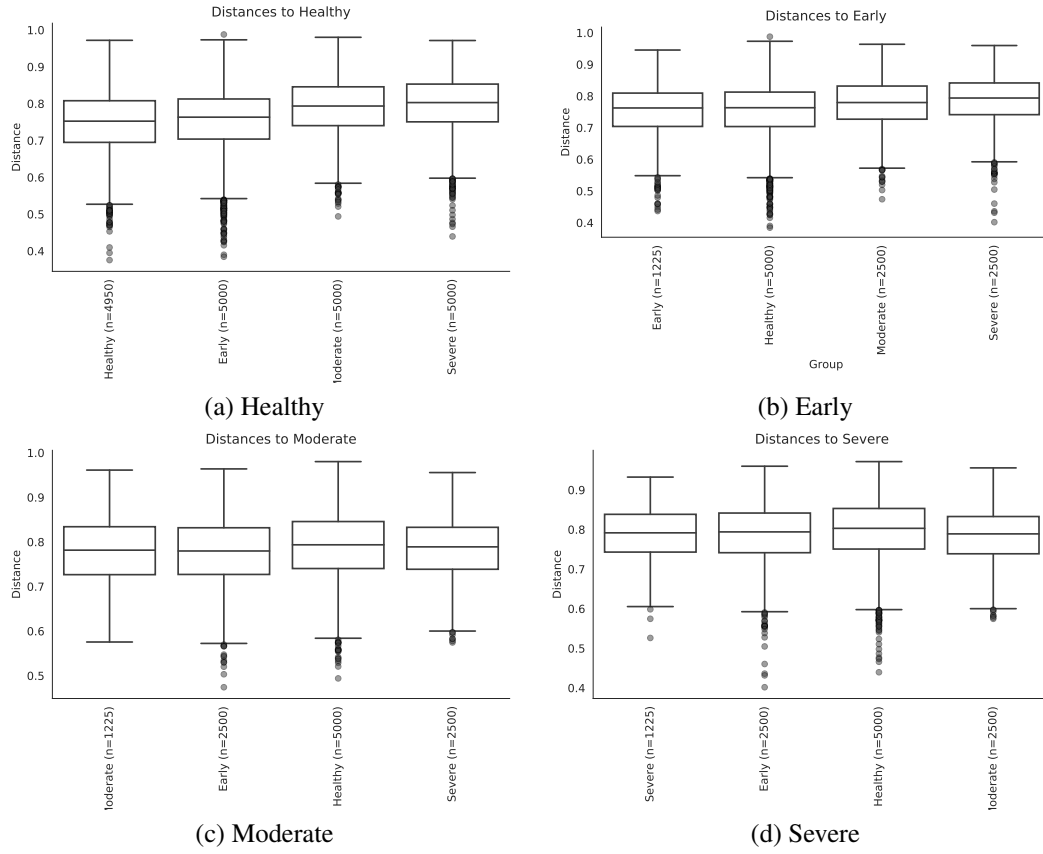
Figure 21: Bray-Curtis Distance Index with DADA2

(a) Healthy
(b) Early
(c) Moderate
(d) Severe
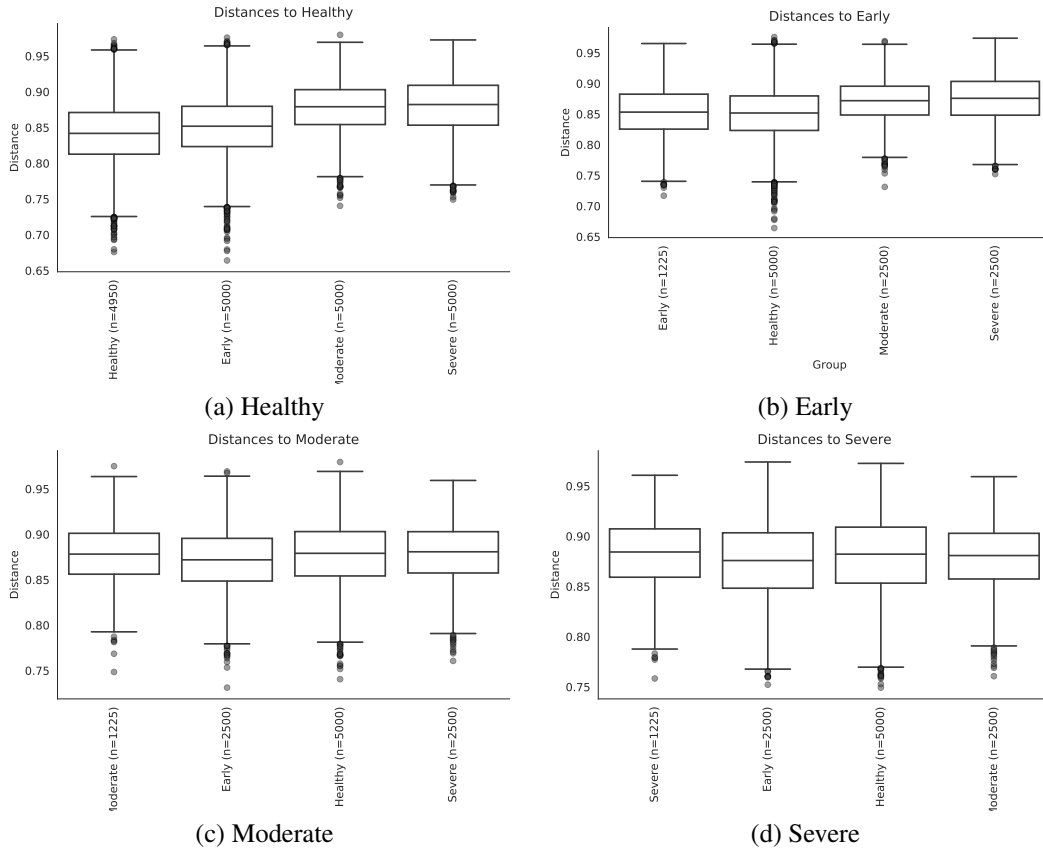
Figure 22: Jaccard Distance Index with DADA2

(a) Healthy

(b) Early

(c) Moderate

(d) Severe

Figure 23: Unweighted Unifrac Distance Index with DADA2

(a) Healthy

(b) Early

(c) Moderate

(d) Severe

Figure 24: Weighted Unifrac Distance Index with DADA2

Table 15: Bray-Curtis Distance Index with Deblur

Group 1	Group 2	Sample size	Permutations	pseudo-F	p-value	q-value
Early	Healthy	150	999	1.7634974220433302	0.019	0.022799999999999997
Early	Moderate	100	999	3.203442604434298	0.001	0.0015
Early	Severe	100	999	4.192790849454974	0.001	0.0015
Healthy	Moderate	150	999	6.953487468508356	0.001	0.0015
Healthy	Severe	150	999	7.5433379986347155	0.001	0.0015
Moderate	Severe	100	999	1.0959020597220626	0.313	0.313

Table 16: Jaccard Distance Index with Deblur

Group 1	Group 2	Sample size	Permutations	pseudo-F	p-value	q-value
Early	Healthy	150	999	1.3701039884255466	0.001	0.0012
Early	Moderate	100	999	2.198029993855521	0.001	0.0012
Early	Severe	100	999	2.237738583770674	0.001	0.0012
Healthy	Moderate	150	999	4.528432929980079	0.001	0.0012
Healthy	Severe	150	999	4.374635292015638	0.001	0.0012
Moderate	Severe	100	999	1.0036296853126103	0.429	0.429

Table 17: Unweighted UniFrac Distance Index with Deblur

Group 1	Group 2	Sample size	Permutations	pseudo-F	p-value	q-value
Early	Healthy	150	999	2.709074154153053	0.003	0.0036
Early	Moderate	100	999	7.547240014264336	0.001	0.0015
Early	Severe	100	999	7.772239667697252	0.001	0.0015
Healthy	Moderate	150	999	19.48285778321118	0.001	0.0015
Healthy	Severe	150	999	20.254907535032658	0.001	0.0015
Moderate	Severe	100	999	1.061788954262309	0.34	0.34

Table 18: Weighted UniFrac Distance Index with Deblur

Group 1	Group 2	Sample size	Permutations	pseudo-F	p-value	q-value
Early	Healthy	150	999	2.0087857905677193	0.088	0.088
Early	Moderate	100	999	5.981646579135783	0.002	0.003
Early	Severe	100	999	16.572566883582837	0.001	0.002
Healthy	Moderate	150	999	9.494764618252377	0.001	0.002
Healthy	Severe	150	999	20.338834647304648	0.001	0.002
Moderate	Severe	100	999	5.026218407543304	0.003	0.0036

(a) Healthy

(b) Early

(c) Moderate

(d) Severe
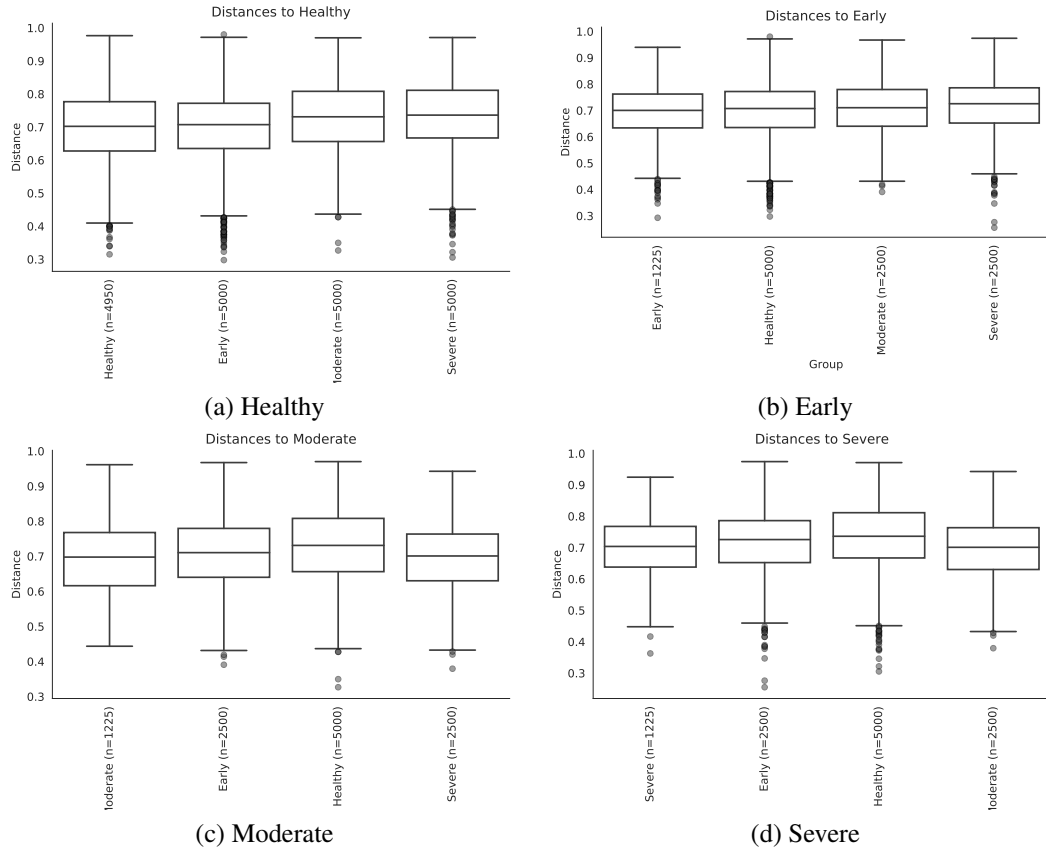
Figure 25: Bray-Curtis Distance Index with Deblur
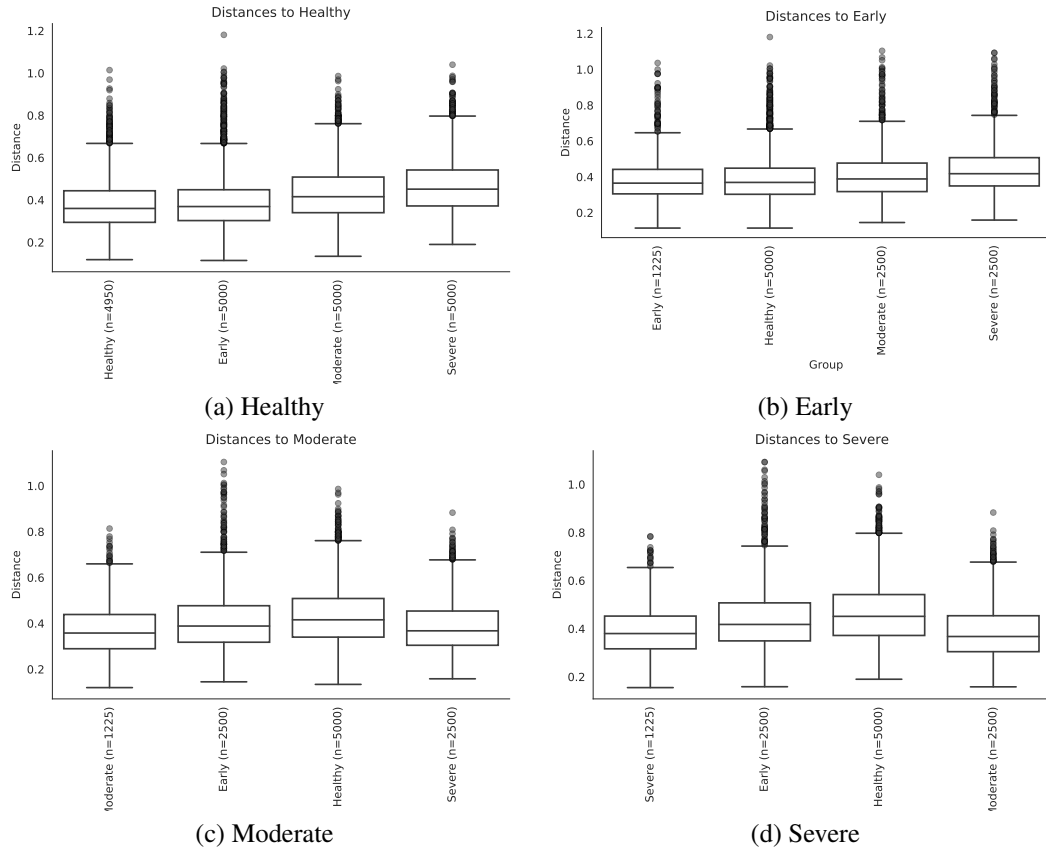

(a) Healthy

(b) Early

(c) Moderate

(d) Severe
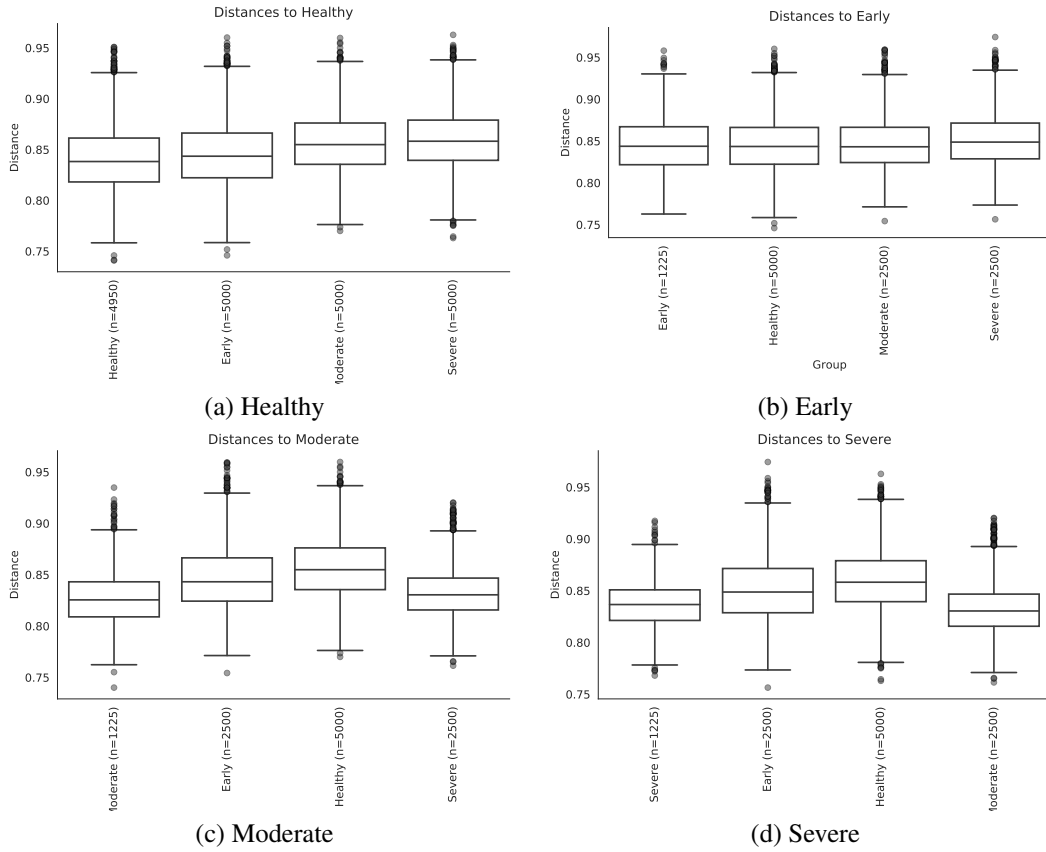
Figure 26: Jaccard Distance Index with Deblur

(a) Healthy

(b) Early

(c) Moderate

(d) Severe
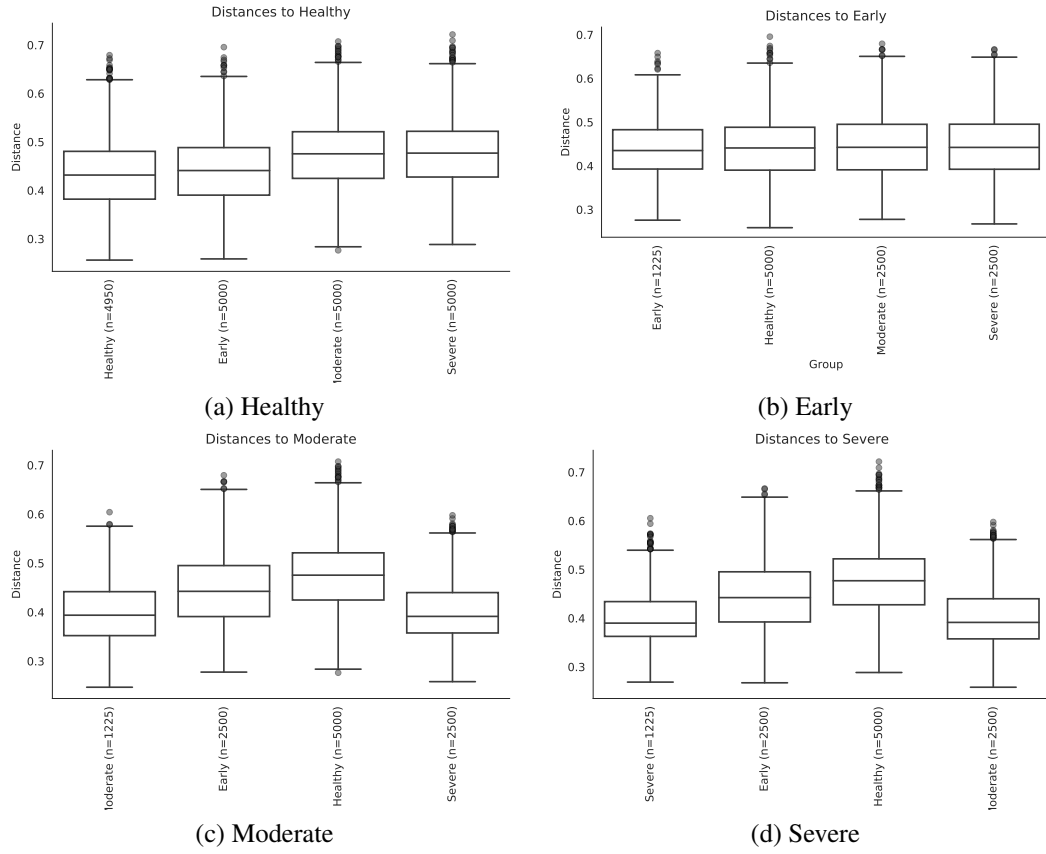
Figure 27: Unweighted Unifrac Distance Index with Deblur

(a) Healthy

(b) Early

(c) Moderate
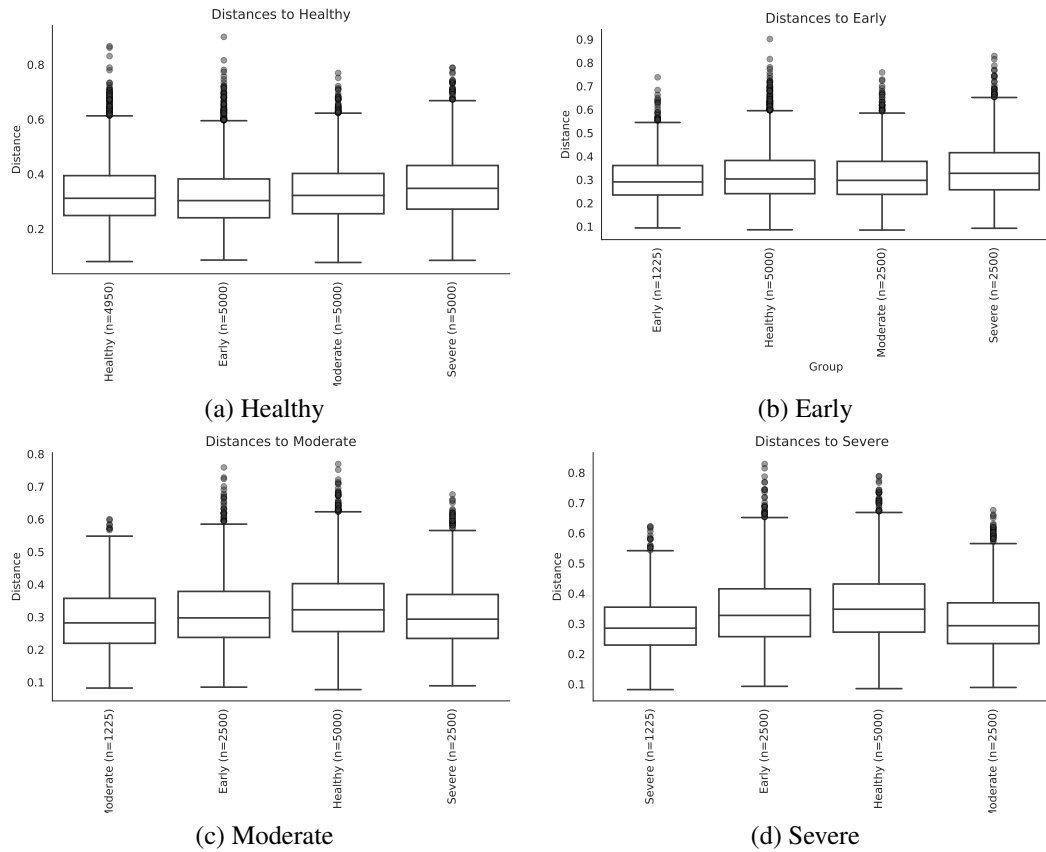
(d) Severe

Figure 28: Weighted Unifrac Distance Index with Deblur

Table 19: ANCOM Significant Taxa with DADA2 and Greengenes

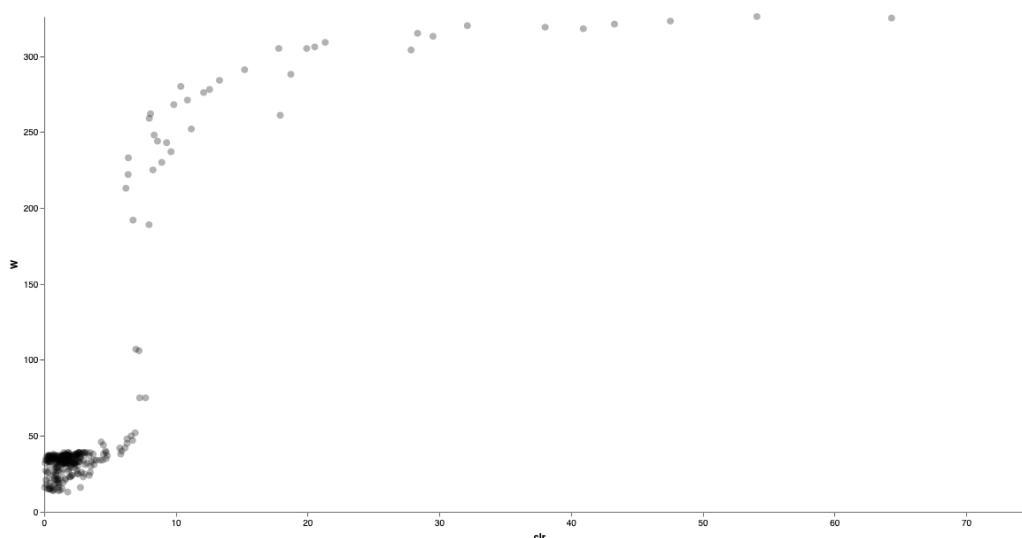|	W	Reject null hypothesis
Bacteria Actinobacteria Actinobacteria Actinomycetales Actinomyc-etaceae Actinomyces	326	True
Bacteria Firmicutes Clostridia Clostridiales Peptostreptococcaceae Fil-ifactor	325	True
Bacteria Spirochaetes Spirochaetes Spirochaetales Spirochaetaceae Treponema	325	True
Bacteria Bacteroidetes Bacteroidia Bacteroidales Prevotellaceae Pre-votella intermedia	323	True
Bacteria Bacteroidetes Bacteroidia Bacteroidales Porphyromonadaceae Porphyromonas endodontalis	321	True
Bacteria Spirochaetes Spirochaetes Spirochaetales Spirochaetaceae Treponema amylovorum	320	True
Bacteria Synergistetes Synergistia Synergistales Dethiosulfovibri-onaceae TG5	319	True
Bacteria Tenericutes Mollicutes Mycoplasmatales Mycoplasmataceae Mycoplasma	318	True
Bacteria Bacteroidetes Bacteroidia Bacteroidales Porphyromonadaceae Tannerella	315	True
Bacteria Bacteroidetes Bacteroidia Bacteroidales Porphyromonadaceae Porphyromonas	313	True
Bacteria Actinobacteria Actinobacteria Actinomycetales Corynebacte-riaceae Corynebacterium durum	309	True
Bacteria Bacteroidetes Bacteroidia Bacteroidales	306	True
Bacteria Firmicutes Clostridia Clostridiales [Mogibacteriaceae]	305	True
Bacteria Proteobacteria Epsilonproteobacteria Campylobacterales Campylobacteraceae Campylobacter	305	True
Bacteria Firmicutes Clostridia Clostridiales [Acidaminobacteraceae]	304	True

Figure 29: ANCOM Volcano Plot with DADA2 and Greengenes

Table 20: ANCOM Significant Taxa with DADA2 and SILVA

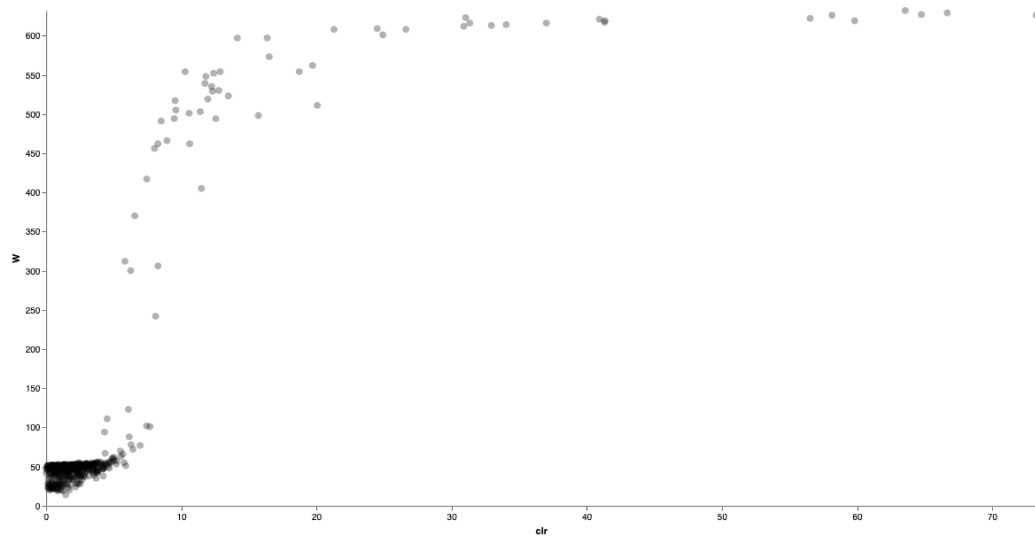|	W	Reject null hypothesis
Bacteria Actinobacteriota Actinobacteria Actinomycetales Actinomycetaceae Actinomyces	632	True
Bacteria Bacteroidota Bacteroidia Bacteroidales Porphyromonadaceae Porphyromonas Porphyromonas gingivalis	629	True
Bacteria Firmicutes Clostridia Peptostreptococcales-Tissierellales Peptostreptococcaceae Filifactor Filifactor alocis	627	True
Bacteria Bacteroidota Bacteroidia Bacteroidales Prevotellaceae Prevotella Prevotella intermedia	626	True
Bacteria Spirochaetota Spirochaetia Spirochaetales Spirochaetaceae Treponema Treponema denticola	626	True
Bacteria Actinobacteriota Actinobacteria Actinomycetales Actinomycetaceae Actinomyces Schaalia odontolytica	623	True
Bacteria Bacteroidota Bacteroidia Bacteroidales Tannerellaceae Tannerella Tannerella forsythia	622	True
Bacteria Spirochaetota Spirochaetia Spirochaetales Spirochaetaceae Treponema Treponema medium	621	True
Bacteria Firmicutes Clostridia Peptostreptococcales-Tissierellales Anaerovoracaceae [Eubacterium] nodatum group [Eubacterium] nodatum	619	True
Bacteria Spirochaetota Spirochaetia Spirochaetales Spirochaetaceae Treponema uncultured bacterium	619	True
Bacteria Firmicutes Bacilli Mycoplasmatales Mycoplasmataceae Mycoplasma Metamycoplasma faucium	617	True
Bacteria Synergistota Synergistia Synergistales Synergistaceae Fretibacterium	616	True
Bacteria Spirochaetota Spirochaetia Spirochaetales Spirochaetaceae Treponema	616	True
Bacteria Firmicutes Clostridia Lachnospirales Defluviitaleaceae Defluviitaleaceae UCG-011 Lachnospiraceae bacterium	614	True
Bacteria Bacteroidota Bacteroidia Bacteroidales Porphyromonadaceae Porphyromonas	613	True
Bacteria Firmicutes Clostridia Peptostreptococcales-Tissierellales Anaerovoracaceae [Eubacterium] brachy group [Eubacterium] brachy	612	True
Bacteria Bacteroidota Bacteroidia Bacteroidales Prevotellaceae	609	True
Bacteria Actinobacteriota Actinobacteria Corynebacteriales Corynebacteriaceae Corynebacterium Corynebacterium durum	608	True
Bacteria Firmicutes Clostridia Peptostreptococcales-Tissierellales Anaerovoracaceae [Eubacterium] saphenum group Eubacterium saphenum	608	True
Bacteria Spirochaetota Spirochaetia Spirochaetales Spirochaetaceae Treponema Treponema maltophilum	601	True
Bacteria Campilobacterota Campylobacteria Campylobacterales Campylobacteraceae Campylobacter Campylobacter showae	597	True
Bacteria Actinobacteriota Actinobacteria Actinomycetales Actinomycetaceae Actinomyces Actinomyces graevenitzii	597	True
Bacteria Firmicutes Clostridia Lachnospirales Lachnospiraceae Oribacterium	573	True

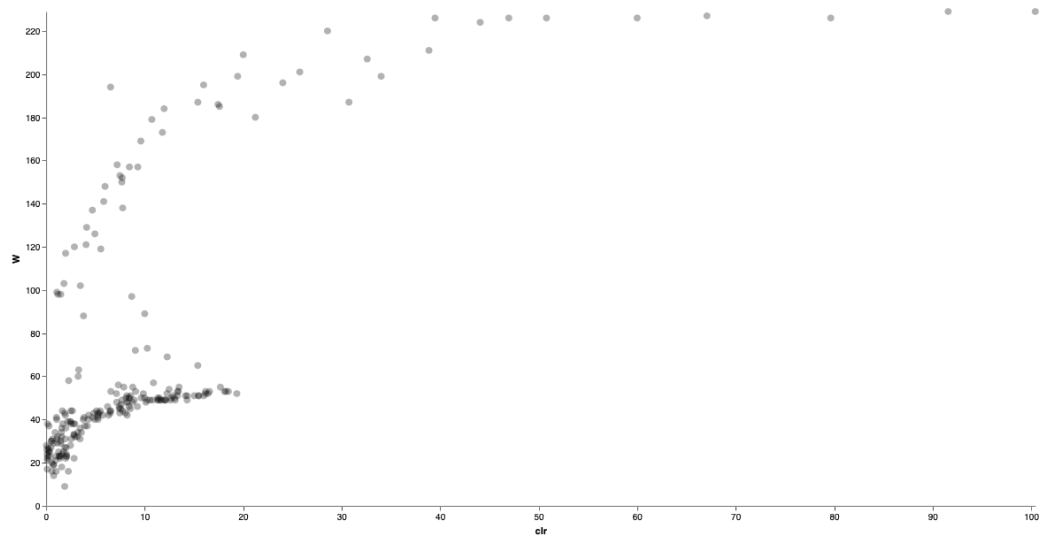Figure 30: ANCOM Volcano Plot with DADA2 and SILVA

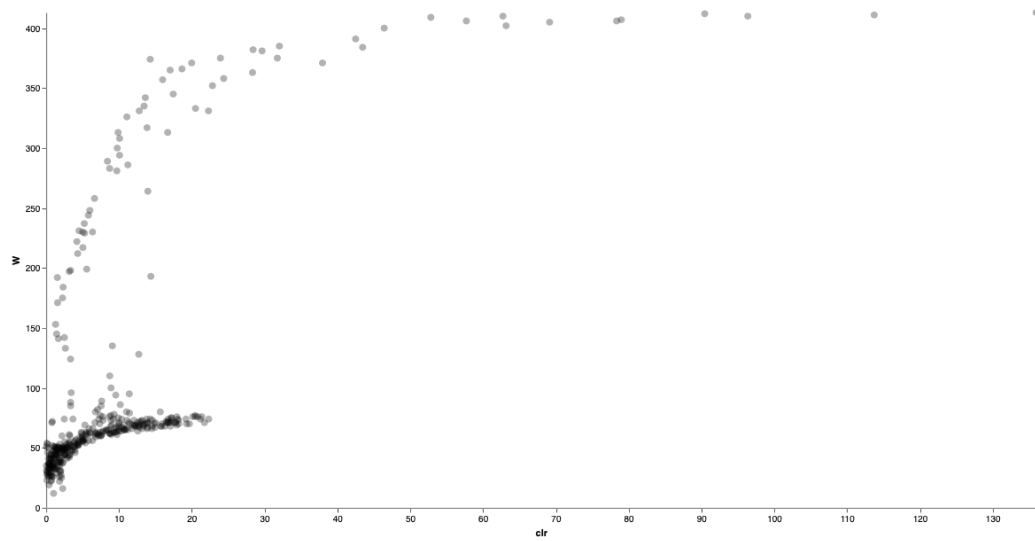Figure 31: ANCOM Volcano Plot with Deblur and Greengenes

Figure 32: ANCOM Volcano Plot with Deblur and SILVA

Table 21: ANCOM Significant Taxa with Deblur and Greengenes

	W	Reject null hypothesis
Bacteria Firmicutes Clostridia Clostridiales Peptostreptococcaceae Filifactor	229	True
Bacteria Spirochaetes Spirochaetes Spirochaetales Spirochaetaceae Treponema	229	True
Bacteria Spirochaetes Spirochaetes Spirochaetales Spirochaetaceae Treponema amylovorum	227	True
Bacteria Bacteroidetes Bacteroidia Bacteroidales Prevotellaceae Prevotella intermedia	226	True
Bacteria Tenericutes Mollicutes Mycoplasmatales Mycoplasmataceae Mycoplasma	226	True
Bacteria Bacteroidetes Bacteroidia Bacteroidales Porphyromonadaceae Porphyromonas endodontalis	226	True
Bacteria Bacteroidetes Bacteroidia Bacteroidales Porphyromonadaceae Tannerella	226	True
Bacteria Synergistetes Synergistia Synergistales Dethiosulfovibrionaceae TG5	226	True
Bacteria Bacteroidetes Bacteroidia Bacteroidales Porphyromonadaceae Porphyromonas	224	True
Bacteria Bacteroidetes Bacteroidia Bacteroidales	220	True
Bacteria Firmicutes Clostridia Clostridiales [Mogibacteriaceae]	211	True
Bacteria Firmicutes Clostridia Clostridiales Peptostreptococcaceae Peptostreptococcus	209	True
Bacteria Proteobacteria Deltaproteobacteria Desulfobacterales Desulfobulbaceae Desulfobulbus	207	True
Bacteria Spirochaetes Spirochaetes Spirochaetales Spirochaetaceae Treponema socranskii	201	True
Bacteria Proteobacteria Epsilonproteobacteria Campylobacterales Campylobacteraceae Campylobacter	199	True
Bacteria Firmicutes Clostridia Clostridiales [Acidaminobacteraceae]	199	True
Bacteria Proteobacteria Gammaproteobacteria Pasteurellales Pasteurellaceae Haemophilus parainfluenzae	196	True
Bacteria Firmicutes Clostridia Clostridiales [Tissierellaceae] Parvimonas	195	True
Bacteria Proteobacteria Betaproteobacteria Neisseriales Neisseriaceae Neisseria subflava	194	True
Bacteria Firmicutes Clostridia Clostridiales [Mogibacteriaceae] Mogibacterium	187	True
Bacteria Actinobacteria Actinobacteria Actinomycetales Actinomycetaceae Actinomyces	187	True
Bacteria Firmicutes Clostridia Clostridiales [Tissierellaceae]	186	True
Bacteria Actinobacteria Actinobacteria Actinomycetales	185	True
Bacteria Firmicutes Clostridia Clostridiales	184	True
Bacteria Firmicutes Clostridia Clostridiales Lachnospiraceae Oribacterium	180	True
Bacteria Firmicutes Clostridia Clostridiales Lachnospiraceae	179	True
Bacteria Bacteroidetes Bacteroidia Bacteroidales Prevotellaceae Prevotella nanceiensis	173	True

Table 22: ANCOM Significant Taxa with DADA2 and SILVA

	W	Reject null hypothesis
Bacteria Actinobacteriota Actinobacteria Actinomycetales Actinomycetaceae Actinomyces	632	True
Bacteria Bacteroidota Bacteroidia Bacteroidales Porphyromonadaceae Porphyromonas Porphyromonas gingivalis	629	True
Bacteria Firmicutes Clostridia Peptostreptococcales-Tissierellales Peptostreptococcaceae Filifactor Filifactor alocis	627	True
Bacteria Bacteroidota Bacteroidia Bacteroidales Prevotellaceae Prevotella Prevotella intermedia	626	True
Bacteria Spirochaetota Spirochaetia Spirochaetales Spirochaetaceae Treponema Treponema denticola	626	True
Bacteria Actinobacteriota Actinobacteria Actinomycetales Actinomycetaceae Actinomyces Schaalia odontolytica	623	True
Bacteria Bacteroidota Bacteroidia Bacteroidales Tannerellaceae Tannerella Tannerella forsythia	622	True
Bacteria Spirochaetota Spirochaetia Spirochaetales Spirochaetaceae Treponema Treponema medium	621	True
Bacteria Firmicutes Clostridia Peptostreptococcales-Tissierellales Anaerovoracaceae [Eubacterium] nodatum group [Eubacterium] nodatum	619	True
Bacteria Spirochaetota Spirochaetia Spirochaetales Spirochaetaceae Treponema uncultured bacterium	619	True
Bacteria Firmicutes Bacilli Mycoplasmatales Mycoplasmataceae Mycoplasma Metamycoplasma faucium	617	True
Bacteria Synergistota Synergistia Synergistales Synergistaceae Fretibacterium	616	True
Bacteria Spirochaetota Spirochaetia Spirochaetales Spirochaetaceae Treponema	616	True
Bacteria Firmicutes Clostridia Lachnospirales Defluviitaleaceae Defluviitaleaceae UCG-011 Lachnospiraceae bacterium	614	True
Bacteria Bacteroidota Bacteroidia Bacteroidales Porphyromonadaceae Porphyromonas	613	True
Bacteria Firmicutes Clostridia Peptostreptococcales-Tissierellales Anaerovoracaceae [Eubacterium] brachy group [Eubacterium] brachy	612	True
Bacteria Bacteroidota Bacteroidia Bacteroidales Prevotellaceae	609	True
Bacteria Actinobacteriota Actinobacteria Corynebacteriales Corynebacteriaceae Corynebacterium Corynebacterium durum	608	True
Bacteria Firmicutes Clostridia Peptostreptococcales-Tissierellales Anaerovoracaceae [Eubacterium] saphenum group Eubacterium saphenum	608	True
Bacteria Spirochaetota Spirochaetia Spirochaetales Spirochaetaceae Treponema Treponema maltophilum	601	True
Bacteria Campilobacterota Campylobacteria Campylobacterales Campylobacteraceae Campylobacter Campylobacter showae	597	True
Bacteria Actinobacteriota Actinobacteria Actinomycetales Actinomycetaceae Actinomyces Actinomyces graevenitzii	597	True
Bacteria Firmicutes Clostridia Lachnospirales Lachnospiraceae Oribacterium	573	True

4.6 t-SNE Plot with Whole Microbiome

As mentioned herein-before, t-SNE is a technique which reduce multi-dimensional data into two-dimension. Whole microbiome data are multi-dimensional data, which have *circa* 600 columns, so the data should be reduced their dimension for readability. Hence, by the grace of t-SNE, the microbiome data have been deflated their dimension: 328 taxa from DADA2 and Greengenes (Figure 33), 633 taxa from DADA2 and SILVA (Figure 34), 232 taxa from Deblur and Greengenes (Figure 35) and 414 taxa from Deblur and SILVA (Figure 36).

4.7 t-SNE Plot with ANCOM Selected Microbiome Data

As whole microbiome data, ANCOM selected microbiome data are also multi-dimensional data, even though their columns are selected by ANCOM. Hence, with t-SNE, ANCOM selected microbiome data have also been deflated their dimension: 15 taxa (as Table 19) from DADA2 and Greengenes (Figure 37), 23 taxa (as Table 20) from DADA2 and SILVA (Figure 38), 27 taxa (as Table 21) from Deblur and Greengenes (Figure 35) and 20 taxa (as Table 22) from Deblur and SILVA (Figure 40).

4.8 RandomForest Classifier

5 Discussion

6 References

Amir, A., McDonald, D., Navas-Molina, J. A., Kopylova, E., Morton, J. T., Xu, Z. Z., . . . others (2017). Deblur rapidly resolves single-nucleotide community sequence patterns. *MSystems*, *2*(2).

Barrett, P., Hunter, J., Miller, J. T., Hsu, J.-C., & Greenfield, P. (2005). matplotlib–a portable python plotting package. In *Astronomical data analysis software and systems xiv* (Vol. 347, p. 91).

Bolyen, E., Rideout, J. R., Dillon, M. R., Bokulich, N. A., Abnet, C., Al-Ghalith, G. A., . . . others (2018). *Qiime 2: Reproducible, interactive, scalable, and extensible microbiome data science* (Tech. Rep.). PeerJ Preprints.

Bolyen, E., Rideout, J. R., Dillon, M. R., Bokulich, N. A., Abnet, C. C., Al-Ghalith, G. A., . . . others (2019). Reproducible, interactive, scalable and extensible microbiome data science using qiime 2. *Nature biotechnology*, *37*(8), 852–857.

Breiman, L. (2001). Random forests. *Machine learning*, *45*(1), 5–32.

Callahan, B. J., McMurdie, P. J., Rosen, M. J., Han, A. W., Johnson, A. J. A., & Holmes, S. P. (2016). Dada2: high-resolution sample inference from illumina amplicon data. *Nature methods*, *13*(7), 581–583.

DeSantis, T. Z., Hugenholtz, P., Larsen, N., Rojas, M., Brodie, E. L., Keller, K., . . . Andersen, G. L. (2006). Green-genes, a chimera-checked 16s rrna gene database and workbench compatible with arb. *Applied and environmental microbiology*, *72*(7), 5069–5072.

Flemmig, T. F. (1999). Periodontitis. *Annals of Periodontology*, *4*(1), 32–37.

Gihawi, A., Rallapalli, G., Hurst, R., Cooper, C. S., Leggett, R. M., & Brewer, D. S. (2019). Sepath: benchmarking the search for pathogens in human tissue whole genome sequence data leads to template pipelines. *Genome biology*, *20*(1), 1–15.

Gill, S. R., Pop, M., DeBoy, R. T., Eckburg, P. B., Turnbaugh, P. J., Samuel, B. S., . . . Nelson, K. E. (2006). Metagenomic analysis of the human distal gut microbiome. *science*, *312*(5778), 1355–1359.

Hunter, J. D. (2007). Matplotlib: A 2d graphics environment. *Computing in science & engineering*, *9*(3), 90–95.

James, F. C., & Rathbun, S. (1981). Rarefaction, relative abundance, and diversity of avian communities. *The Auk*, *98*(4), 785–800.

Maaten, L. v. d., & Hinton, G. (2008). Visualizing data using t-sne. *Journal of machine learning research*, *9*(Nov), 2579–2605.

Mandal, S., Van Treuren, W., White, R. A., Eggesbø, M., Knight, R., & Peddada, S. D. (2015). Analysis of composition of microbiomes: a novel method for studying microbial composition. *Microbial ecology in health and disease*, *26*(1), 27663.

McKinney, W., et al. (2011). pandas: a foundational python library for data analysis and statistics. *Python for High Performance and Scientific Computing*, *14*(9).

Olsen, G. J., & Woese, C. R. (1993). Ribosomal rna: a key to phylogeny. *The FASEB journal*, *7*(1), 113–123.

Pedregosa, F., Varoquaux, G., Gramfort, A., Michel, V., Thirion, B., Grisel, O., . . . others (2011). Scikit-learn: Machine learning in python. *the Journal of machine Learning research*, *12*, 2825–2830.

Pruesse, E., Quast, C., Knittel, K., Fuchs, B. M., Ludwig, W., Peplies, J., & Glöckner, F. O. (2007). Silva: a comprehensive online resource for quality checked and aligned ribosomal rna sequence data compatible with arb. *Nucleic acids research*, *35*(21), 7188–7196.

Turnbaugh, P. J., Ley, R. E., Hamady, M., Fraser-Liggett, C. M., Knight, R., & Gordon, J. I. (2007). The human microbiome project. *Nature*, *449*(7164), 804–810.
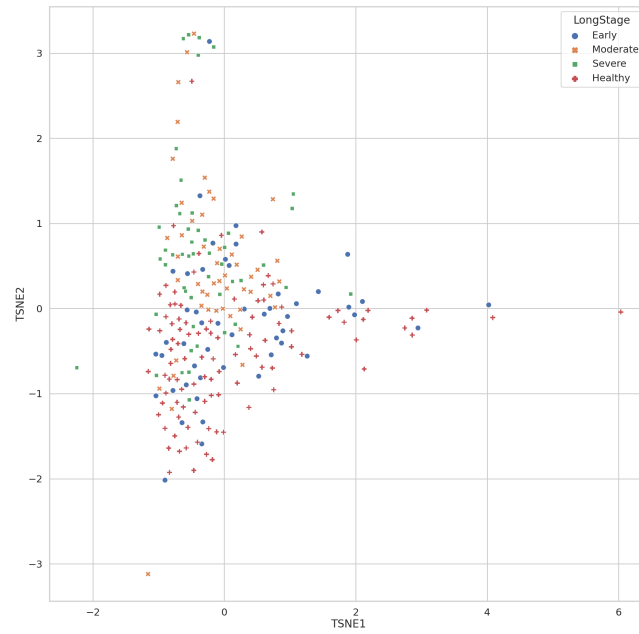
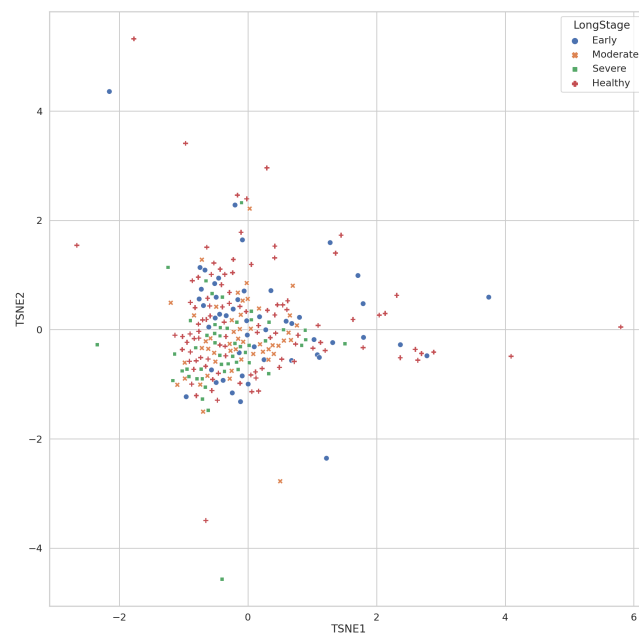Figure 33: t-SNE Plot with Whole Microbiome from DADA2 and Greengenes

Figure 34: t-SNE Plot with Whole Microbiome from DADA2 and SILVA
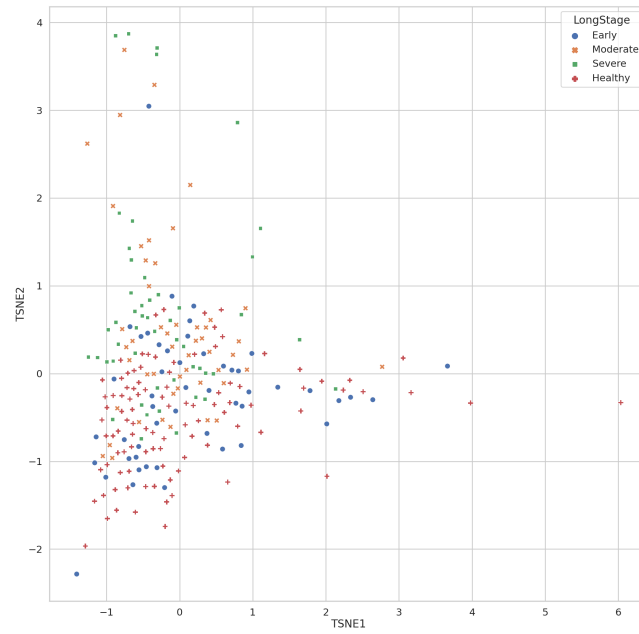
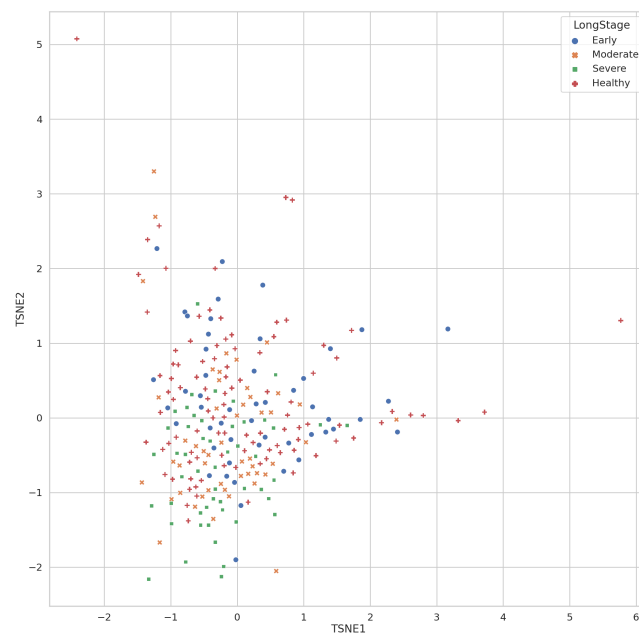Figure 35: t-SNE Plot with Whole Microbiome from Deblur and Greengenes

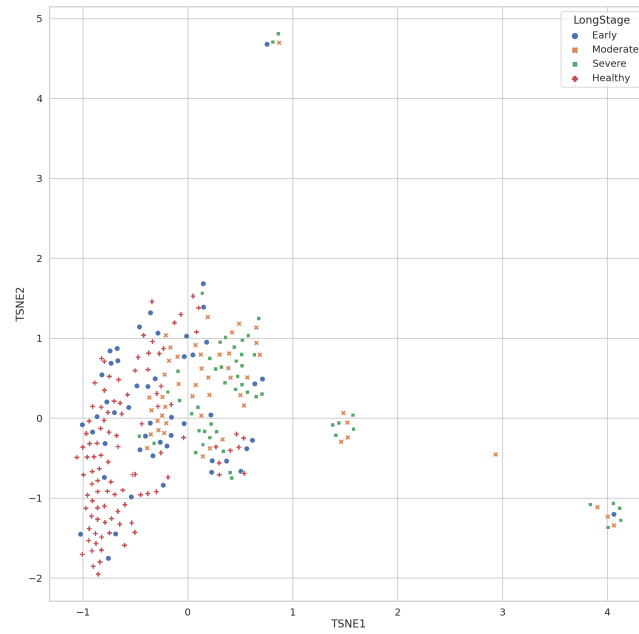Figure 36: t-SNE Plot with Whole Microbiome from Deblur and SILVA

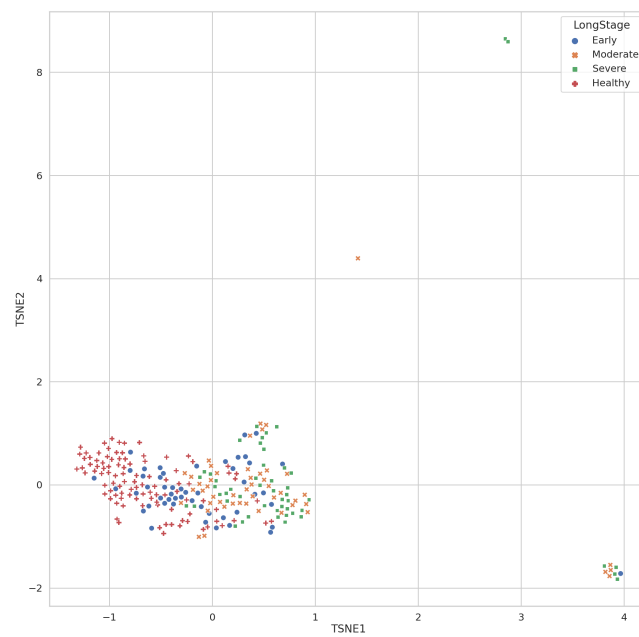Figure 37: t-SNE Plot with ANCOM Selected Microbiome Data from DADA2 and Greengenes

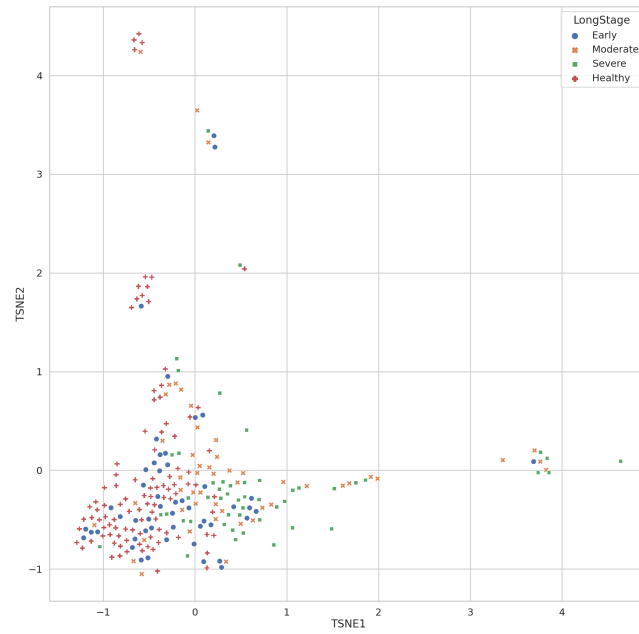Figure 38: t-SNE Plot with ANCOM Selected Microbiome Data from DADA2 and SILVA

Figure 39: t-SNE Plot with ANCOM Selected Microbiome Data from Deblur and Greengenes
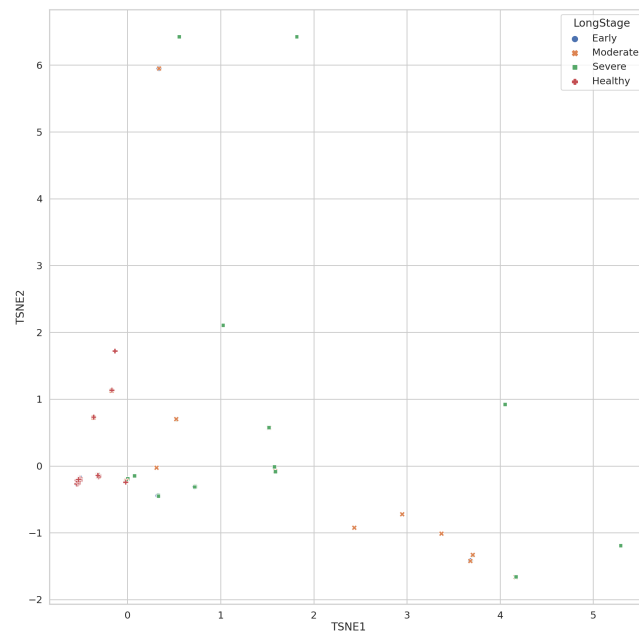

Figure 40: t-SNE Plot with ANCOM Selected Microbiome Data from Deblur and SILVA

Van Dyke, T. E., & Dave, S. (2005). Risk factors for periodontitis. *Journal of the International Academy of Periodontology*, *7*(1), 3.

Waskom, M., & the seaborn development team. (2020, September). *mwaskom/seaborn.* Zenodo. Retrieved from `https://doi.org/10.5281/zenodo.592845` doi: 10.5281/zenodo.592845

Weiss, S., Xu, Z. Z., Peddada, S., Amir, A., Bittinger, K., Gonzalez, A., . . . others (2017). Normalization and microbial differential abundance strategies depend upon data characteristics. *Microbiome*, *5*(1), 27.